

1 Development of a papillation assay using constitutive promoters to find
2 hyperactive transposases

3

4 Michael Tellier^{2*} and Ronald Chalmers^{1*}

5

6 *Corresponding authors: michael.tellier@path.ox.ac.uk,

7 ronald.chalmers@nottingham.ac.uk,

8

9 ¹ School of Life Sciences, University of Nottingham, Queen's Medical Centre,
10 Nottingham, NG7 2UH, UK

11 ² Current address: Sir William Dunn School of Pathology, University of Oxford,
12 Oxford, OX1 3RF, UK

13

14

15

16

17

18

19

20

21

22

23

24

25

26 **Abstract**

27 Background

28 Transposable elements is an extremely diverse group of genetic elements
29 encoding their own mobility. This ability has been exploited as a powerful tool
30 for molecular biology and genomics techniques. However, transposition
31 activity is regulated by *cis* and/or *trans* mechanisms because of the need to
32 co-exist with their host. This represents a limitation to their usage as
33 biotechnological tools. The development of screening assays and the
34 improvement of current ones is therefore needed to find hyperactive
35 transposases.

36 Results

37 We present in this study an improvement of the well-known papillation assay
38 where in place of an inducible promoter, we designed a set of constitutive
39 promoters cloned into a one or five copies vector in presence or absence of a
40 ribosome binding site. This set of vectors provides a wide range of
41 transposase expression and offers a more uniform expression of the
42 transposase across cells compared to inducible promoters. These constructs
43 can therefore be used to screen for hyperactive transposases or for
44 transposases resistant to overproduction inhibition, a mechanism affecting
45 DNA transposases such as Hsmar1, which decreases the transposition rate
46 when the transposase concentration increases. We characterized and
47 validated our set of vectors with the Hsmar1 transposase and took advantage
48 of our approach to investigate the effects on the transposition rate of inserting
49 mutations in the Hsmar1 dimer interface or of covalently binding two Hsmar1
50 monomer.

51 Conclusions

52 This improved papillation assay should be applicable to a wide variety of DNA
53 transposases. It also provides a straightforward approach to screen
54 transposase mutant libraries with a specific expression level to find
55 hypoactive, hyperactive or overproduction inhibition resistant transposases.
56 Our approach could also be useful for synthetic biology as a combination of
57 the wild type or covalently bound Hsmar1 transposase with a library of weak
58 promoters offers the possibility to find promoters expressing on average one
59 or two proteins per cell.

60

61

62

63

64

65

66

67

68

69

70

71

72

73

74 Key words: transposon; transposase; overproduction inhibition; papillation

75 assay; Hsmar1

76 **Background**

77 Transposable elements (TEs) are DNA sequences encoding their own ability
78 to move in a genome from one place to another. They are found in virtually all
79 organisms and are particularly present in eukaryotes where they can
80 represent a high percentage of the genome (1-3). Originally described as
81 selfish elements due to their ability to replicate independently of their host,
82 TEs have now been shown to be important drivers of genome evolution (4, 5).
83 Indeed, TEs can provide novel transcription factors binding sites, promoters,
84 exons or poly(A) sites and can also be co-opted as micro RNAs or long
85 intergenic RNAs (6-8).
86 TEs are therefore a diverse group of DNA sequences using a wide range of
87 mechanisms to transpose inside and between hosts. For example, some DNA
88 transposons like the *mariner* elements transpose through a “cut and paste”
89 mechanism where a single copy of the transposon moves from one place to
90 another without copying itself (9). Over the past several years, our group and
91 others have described the mechanisms regulating the transposition rate of
92 different DNA transposases, such as Hsmar1 or Mos1 (10-15). In Hsmar1, the
93 central regulatory mechanism of transposition is overproduction inhibition
94 (OPI) (16), a phenomenon emerging from the decreased binding affinity of a
95 transposase dimer for the second end of the transposon after binding the first
96 end (10). This decreased affinity increases the probability of another Hsmar1
97 dimer to bind the free end, blocking transposition at the same time. Thus, OPI
98 curbs the transposition of Hsmar1 to avoid an exponential transposition rate
99 which would prove catastrophic for the host (12).

100 However, OPI represents a limitation in the development of hyperactive
101 transposases, which are for example needed for transposon mutagenesis.
102 Several approaches can be used to overcome OPI such as modifying the
103 binding kinetics of the transposase to the ITR or the monomer-dimer
104 equilibrium. Indeed, we and others previously shown that most mutations in
105 the conserved WVPHEL motif in Himar1 and Hsmar1, which is involved in the
106 subunit interface, result in hyperactive transposases but at the cost of
107 producing nonproductive DNA double-strand breaks and therefore DNA
108 damage (17, 18).

109 The discovery of hyperactive transposases in bacteria has mostly been
110 accomplished by screening libraries of transposase mutants with the
111 papillation assay (Supplementary Figure 1a) (19, 20). This assay is based on
112 a promoter-less lacZ gene flanked by transposon ends. This reporter is
113 integrated in a silent region of the genome of *Escherichia coli*. The
114 transposase gene is provided *in trans* on a plasmid to simplify mutagenesis
115 and library handling. Transposition events into an expressed ORF give rise to
116 lacZ gene fusion proteins. When this happens within a colony growing on an
117 X-gal indicator plate, it converts the cell to a lac+ phenotype, which allows the
118 outgrowth of a blue microcolony (papillae) on a background of white cells. The
119 transposition rate is given by the number of papillae per colony and by the
120 rate of their appearance. The visual read-out of this assay simplifies the
121 screening of mutant libraries for discovering hypo- or hyper-active
122 transposases. The mating-out assay is a more quantitative assay using the
123 same reporter strain. Here, the rate of transposition is measured by

124 movement of the reporter from its chromosomal location into a conjugative
125 plasmid.
126 In the current work, we present an improvement of the papillation assay by
127 using a set of constitutive promoters cloned in a single or five copies vector in
128 absence or presence of a ribosome binding site (RBS). This set of expression
129 vectors allows us to express a transposase across a wide range of expression
130 level facilitating the screening of hyperactive and/or OPI-resistant
131 transposases. We used this set of vectors to compare an Hsmar1 monomer to
132 a covalently bound Hsmar1 dimer and to test for hyperactivity and OPI-
133 resistance several Hsmar1 mutants. We found that one Hsmar1 mutant in the
134 dimer interface, R141L, is resistant to OPI in *E. coli*.

135

136 **Results**

137 **Characterization of the constitutive promoters**

138 The papillation assay provides a visual assessment of the transposition rate,
139 which can be determined from the rate of papillae apparition and their number
140 per colony (19). The transposition rate is dependent of the concentration and
141 the activity of the transposase (12). Conventionally, transposition assays use
142 inducible promoters which limits the accessible range of transposase
143 expression and also result in cell-to-cell variability due to the unequal diffusion
144 of the inducer in colonies. To overcome these limitations, we synthesized a
145 set of five constitutive promoters (00, JJ, K, E, and W) based on (21). In
146 addition, we created a null-expression vector by replacing the promoter and
147 the RBS with a featureless, undistorted, DNA sequence consisting of a single
148 repeat of the tetranucleotide (GACT)_{n=44}. To increase the range of expression

149 levels obtainable, we also created a variant of each promoter where the RBS
150 has been abolished. The expression construct is shown in Figure 1A and is
151 composed of the promoter and a RBS sequence, an NdeI and BamHI
152 restriction sites to clone a gene of interest which can then be fused to a C-
153 terminal 3x FLAG tag. To avoid any read-through transcription, the construct
154 is flanked by terminator sequences. The expression constructs were cloned
155 either into a one-copy vector or a five-copy vector, pBACe3.6 and pGHM491,
156 respectively. The following nomenclature will be used: Bp1 to Bp6 represents
157 the six promoters cloned into the single copy vector, lp1 to lp6 corresponds to
158 the six promoters cloned into the five copy vector, the '-' and '+' represents
159 the absence or the presence of a RBS, respectively, while the 'N' corresponds
160 to the RBS composed of the GACT repeat in the p1 promoter.

161 We first determined the strength of each expression vector by inserting an
162 *EGFP* gene in each vector to investigate by flow cytometry the amount of
163 fluorescence produced (Figure S1B). To rank the expression vectors, we
164 normalize their average fluorescence value against the strongest vector, lp6+
165 (Figure 1B). Most of the one-copy expression vectors produce an amount of
166 EGFP close to the detection threshold and therefore their ranking might not
167 be representative. However, we can observe that the five-copy expression
168 vectors produce more fluorescence than the one-copy vectors and that the
169 vectors with a consensus RBS are also producing more fluorescence than the
170 vectors without a RBS motif, except for the p1 promoter where the presence
171 or absence of the RBS does not influence the amount of fluorescence
172 produced. We confirmed the flow cytometry results for the strongest
173 expression vectors expressing Hsmar1 by performing western blot with an

174 anti-Hsmar1 antibody (Figure 1C). We also compared by western blotting
175 these constructs with the inducible promoter normally used for papillation
176 assay, the pTac promoter (Figure 1D). Interestingly, two of our constructs
177 (Ip5+ and Ip6+) produce a higher amount of Hsmar1 than the pTac promoter
178 fully induced with 1 mM of IPTG.

179

180 **Characterization of the papillation assay with the wild-type Hsmar1** 181 **transposase**

182 To characterize the implementation of the constitutive promoters into the
183 papillation assay, we used the wild-type Hsmar1 transposase as we have
184 already well characterized its activity in papillation assay (18). We defined the
185 transposition rate as the average number of papillae per colony after five days
186 of incubation at 37°C. Bacterial cells stop dividing after a few days at 37°C
187 because of carbon exhaustion, therefore affecting the number of visible
188 papillae since late transposition events, i.e. a few divisions before the cells
189 stop dividing because of carbon exhaustion, will not be visible because of the
190 insufficient number of division. To overcome this limitation, we took advantage
191 of the fact that bacterial cells having undergone a transposition event resulting
192 in a fusion between a host gene and the lacZ gene, located in the transposon,
193 will be able to use lactose as a carbon source. Thus, by adding lactose to the
194 medium we should recover a higher number of papillae per colony since the
195 lac⁺ cells resulting from a late transposition event would be able to continue to
196 grow by using lactose (Supplementary Figure 2). Indeed, by using the Ip3+
197 expression vector and a range of lactose concentration, we observed a
198 correlation between the number of papillae per colony and the lactose

199 concentration (Supplementary Figure 2A/ to C/). We decided to use a
200 concentration of lactose of 0.1% for the papillation assay since it is
201 representing the best trade-off between the number of papillae per colony and
202 the size of the papillae to allow a proper quantitation at high transposition rate.
203 We next investigated the transposition rate of each expression vector with the
204 wild-type Hsmar1 transposase. Representative colony of the papillation assay
205 for each Hsmar1 expression vectors is shown in Figure 2A and their
206 respective whole plate pictures are shown in Supplementary Figure 3. As
207 expected from the wide-range of expression, we observed a 200-fold variation
208 in the average number of papillae per colony as the quantitation of the
209 different expression vectors shows in Figure 2B. To better visualize the
210 relationship between the expression vector strength and the transposition
211 rate, determined by the number of papillae per colony, we plotted the vector
212 strength determined by flow cytometry (Figure 1B) against the number of
213 papillae per colony (Figure 2C). As previously published *in vitro*, in *E. coli* and
214 in HeLa cells, the wild-type Hsmar1 transposase follows an inverse-
215 exponential relationship between transposase expression and transposition
216 rate (12, 22). Interestingly, the transposition rate peaks with the weakest
217 promoters in the single copy vector indicating that the transposition rate is
218 extremely sensitive to overproduction inhibition (OPI) resulting from a slight
219 increase in the transposase concentration. However, for the expression
220 vectors with a similar average promoter strength but a transposition rate
221 below the highest one we cannot determine whether their suboptimal
222 transposition rate is due to an insufficient amount of Hsmar1 transposase in
223 the cell or OPI.

224 Importantly, the transposition assay also provides a more precise approach to
225 investigate weak promoter strength than flow cytometry with EGFP. Indeed,
226 out of the 18 expression vectors having a relative promoter strength around
227 4% of Ip6+, the transposition assay shows a 10-fold change in transposition
228 rate within this set of vectors (Figure 2C).

229

230 **Bounding covalently two Hsmar1 monomers in a dimer affects the**
231 **transposition rate**

232 We recently published a new Hsmar1 construct where two monomers are
233 covalently bound by a linker region (Figure 3A) (23). We use advantage of our
234 approach to test whether the transposition rate of a covalently bound Hsmar1
235 dimer differs to the Hsmar1 monomer. At low expression level, we expect a
236 covalently bound Hsmar1 dimer to transpose more efficiently than an Hsmar1
237 monomer because of the physical link in the covalent dimer, which keeps both
238 monomers close to each other, and also because the covalent dimer requires
239 a single translation event whereas the monomer requires two. We cloned the
240 monomeric and dimeric construct in a set of expression vectors spanning from
241 very low to high expression and performed a papillation assay.

242 Representative colony of the papillation assay of each expression vectors is
243 shown in Figure 3B and their respective whole plate pictures are shown in
244 Supplementary Figure 4. Interestingly, we observe a change in the number of
245 papillae per colony with the lowest expression vectors, as shown by the
246 quantitation in Figure 3C. When compared to the results obtained with
247 Hsmar1 monomer, the covalent dimer transposition rate peaks at a different
248 set of expression vectors, Bp2- and Bp3- for the covalent dimer and Ip2- and

249 Ip1+ for the monomer. These four expression vectors have a similar relative
250 promoter strength, around 4% of Ip6+, indicating that the number of
251 transposases expressed per cell is particularly low (see Discussion).
252 Inversely, we do not observe any difference in the number of papillae per
253 colony with stronger expression vectors such as Ip3+ and Ip6+ (Figure 3B to
254 D). This indicates that a covalently bound Hsmar1 dimer is as sensitive to OPI
255 as the monomer, which is also supported by the inverse relationship between
256 the average promoter strength and the transposition rate for both the
257 monomer and the covalent dimer (Figure 3D).

258

259 **SETMAR transposition activity was lost during the same period than**

260 **Hsmar1 transposase domestication**

261 The Hsmar1 transposase was originally found in the human genome where
262 an Hsmar1 transposase with several mutations is fused to a SET domain to
263 form SETMAR (24-26). The domesticated Hsmar1 transposase is inefficient at
264 performing transposition because of the mutation of the last DDD triad
265 catalytic motif to a DDN (25, 26). In addition to the D282N mutation, we
266 performed a papillation assay with a non-induced pTac promoter the 22 other
267 mutations present in the human SETMAR to determine their effects on
268 Hsmar1 transposition (Figure 4A). Most of the mutations present in the human
269 SETMAR occurred outside the DNA binding domain and happened at the
270 same time as the domestication of the Hsmar1 transposase. Representative
271 colony of the papillation assay of each expression vectors is shown in Figure
272 4B and their respective whole plate pictures are shown in Supplementary
273 Figure 5. In addition to D282N, two other mutations, C219A and S279L,

274 disrupt completely Hsmar1 transposition activity. Two other mutations located
275 in the DNA binding domain, E2K and R53C, affect severely the transposition
276 rate. In addition, seven other mutations located mostly in the catalytic domain
277 mildly affect Hsmar1 transposition activity. Only one mutation, V201L,
278 increases Hsmar1 transposition rate whereas the remaining mutations were
279 neutral. Interestingly, nearly all deleterious mutations for transposition arose
280 at the same time as the domestication of the Hsmar1 transposase.

281

282 **Mutations in Hsmar1 dimer interface produce hyperactive mutants in** 283 **bacteria**

284 The mutagenic nature of transposable elements make them useful in
285 screening for essential genes. However, OPI limits the transposition rate
286 when the transposase concentration is too high (12). One way to overcome
287 OPI is to decrease the stability of the Hsmar1 dimer to shift the monomer-
288 dimer equilibrium to the inactive monomeric form. We decided to take
289 advantage of our approach to investigate two Hsmar1 transposases mutated
290 in the dimer interface, one known mutant, F132A (F460 in SETMAR (27)) and
291 a novel one R141L (9). We used three vectors expressing Hsmar1 at a low
292 (Bp1+), optimal (Ip1+) and high (Ip6+) level. Representative colony of the
293 papillation assay of each expression vectors is shown in Figure 4C and their
294 respective whole plate pictures are shown in Supplementary Figure 6. The
295 average number of papillae per colony is indicated below each representative
296 colony. Interestingly, both F132A and R141L transposases are hyperactive at
297 low and optimal levels of expression when compared to WT. A higher
298 transposition rate is also observed at high expression level for both mutants,

299 with R141L showing a stronger resistance to OPI than F132A. To confirm the
300 papillation assay, the mutants' transposition rate was also determined using
301 the mating-out assay, a more quantitative assay measuring the transposition
302 rate through the movement of the transposon reporter from its chromosomal
303 location into a conjugative plasmid (Table 1). The results of the mating-out
304 and transposition assays were similar. Interestingly, Hsmar1 R141L
305 transposition rate is not affected by the high transposase expression level
306 produced by Ip6+, as the rate remains similar between Ip1+ and Ip6+
307 whereas we observe a 147 fold decrease for the wild type transposase and a
308 17 fold decrease for the F132A mutant.
309

Construct	Transposition frequency	Mutant/W.T.
Ip1+ W.T.	$4.73 (\pm 1.02) \times 10^{-5}$	
Ip1+ F132A	$9.73 (\pm 4.53) \times 10^{-4}$	21
Ip1+ R141L	$2.42 (\pm 1.68) \times 10^{-4}$	5
Ip6+ W.T.	$3.22 (\pm 1.02) \times 10^{-7}$	
Ip6+ F132A	$5.79 (\pm 2.63) \times 10^{-5}$	180
Ip6+ R141L	$3.24 (\pm 1.43) \times 10^{-4}$	1006

310 **Table 1: Transposition frequencies of two Hsmar1 transposase mutants**
311 **expressed at optimal and high level.** The bacterial mating-out assays have been
312 done with the RC5097 strain and the Ip1+ or Ip6+ vectors. Transposition frequencies
313 are the average of three independent experiments \pm standard error of the mean.

314

315 **Discussion**

316 We present here an improvement of the papillation assay using a set of
317 constitutive promoters cloned into a single- or five-copies vector in absence or
318 presence of a RBS. This range of expression vectors give us a better control
319 of the transposase expression compared to inducible vectors such as the
320 pTac. This is illustrated in Figure 2C where we observe a large variation in the
321 number of papillae per colony across expression vectors producing EGFP
322 fluorescence close to the background level. This indicates that the
323 transposition rate is extremely sensitive to small variation in transposase
324 concentration, in agreement with previous works from our group (10, 12).

325

326 We recently published a covalently bound Hsmar1 construct, where a single
327 transcription and translation event is sufficient to synthesize an active Hsmar1
328 dimer (23). At low expression level, a change in the transposition rate is
329 observed for the covalent dimer construct when compared to the monomeric
330 construct whereas at higher expression level, the transposition rates are quite
331 similar indicating that OPI is occurring for both the monomer and the covalent
332 dimer Hsmar1 (Figure 3C and D). The change in transposition rate at low
333 expression level is expected because a single translation event is needed for
334 producing a covalently bound Hsmar1 dimer whereas the wild type Hsmar1
335 requires two translation events for producing an active transposase. Based on
336 this idea, we can hypothesize that Bp2- and Bp3-, which provides the highest
337 transposition rates for the covalent dimer, corresponds to weaker promoters
338 than Ip2- and Ip1+, which provides the highest transposition rates for the
339 monomeric Hsmar1 but lower transposition rate for the covalent dimer. Thus,
340 Bp2- and Bp3- are likely to express on average less than two proteins per cell,

341 which is not sufficient to optimally promote transposition for the Hsmar1
342 monomer construct, whereas Ip2- and Ip1+ are likely to express on average
343 at least two proteins per cell, which starts to promote OPI for the covalent
344 dimer construct and therefore results in a lower transposition rate than Bp2-
345 and Bp3-.

346

347 A peculiarity of the Hsmar1 transposase is the presence in anthropoid
348 primates of SETMAR, a gene with new functions in gene regulation resulting
349 from the fusion between a SET gene and an Hsmar1 transposase (24)
350 (Tellier, M. and Chalmers, R., manuscript under review). It was shown that the
351 domesticated Hsmar1 transposase DNA binding domain was under purifying
352 selection whereas the catalytic domain was evolving under neutral selection,
353 with a mutation of the last D of the catalytic triad DDD to an N abolishing
354 SETMAR transposase activity (24-26). In addition to the mutation in the
355 catalytic triad, the domesticated Hsmar1 contains 22 other mutations with
356 three of them located in the DNA binding domain (E2K, R53C and D98N)
357 (Figure 4A and B). Out of the 23 mutations, only one was found to increase
358 the transposition rate in the papillation assay, V201L, whereas 12 mutations
359 were deleterious for the transposition rate with three of them abolishing it
360 completely (C219A, S279L and D282N). Interestingly, 11 of the 12 deleterious
361 mutations occurred at the same time as Hsmar1 was domesticated, resulting
362 in the abolition of SETMAR ability to promote transposition, and are therefore
363 common to all anthropoid primates. Two of the DNA binding mutants, E2K
364 and R53C, are deleterious to Hsmar1 transposition activity in a papillation
365 assay. It will be interesting to determine whether this effect is mediated

366 through a change in ITR binding efficiency, which could have modified
367 SETMAR's ability to bind ITRs in the genome and therefore its emerging
368 functions in regulating gene expression.

369

370 Transposases have become an important and versatile biotechnological tool
371 (28-30). The creation of hyperactive transposases can be advantageous over
372 its wild-type counterpart as for transposon mutagenesis for example. One of
373 the major mechanism limiting the transposition rate of *mariner* transposases is
374 OPI, which is occurring when there is an excess of transposase dimer per
375 transposon (11, 12). We previously show that mutating the conserved
376 WVPHEL motif, which is part of the Hsmar1 transposase dimer interface,
377 resulted in mostly hyperactive transposases (18, 31). Here we show that the
378 mutation of the residues F132 and R141, which are located in the subunit
379 interface (9, 27), also produces hyperactive transposases in *E. coli* with the
380 R141L mutant being OPI-resistant (Figure 4C and Table 1). The hyperactivity
381 of F132A and R141L mutants could be explained by the promotion of one of
382 the conformational change essential for transposition (11). The decreased
383 OPI-sensitivity could result from a decrease in the dimer stability, which shifts
384 the monomer-dimer equilibrium towards the monomeric form, and therefore
385 reduces the concentration of active transposases in the cell. Also, an unstable
386 dimer bound to a transposon end could be more likely to fall apart allowing the
387 recruitment of the previously bound end by another bound dimer, activating
388 transposition. This type of mutant is more likely to be found hyperactive only
389 in bacteria. Indeed, in mammalian cells the size of the nucleus and the bigger
390 ratio of non-specific DNA to specific DNA, i.e. the transposon ends account

391 for a smaller fraction of the genome, will increase the time necessary for a
392 transposase to find a transposon end. Therefore, transposases with a
393 weakened dimer interface are more likely to revert to an inactive monomeric
394 state resulting in hypoactive mutants.

395

396 An unexpected outcome of our range of expression vectors is the realization
397 that the transposition rate could be used as a better approach than EGFP
398 fluorescence to compare the strength of a series of weak promoters. This is
399 illustrated in Figure 1B where 18 of our expression vectors have a relative
400 promoter strength comprised between 3 and 4% of Ip6+, our strongest vector.
401 However, in Figure 2C, we observe a 10-fold difference in the transposition
402 rate between these 18 expression vectors. It is interesting to note that the
403 seven expression vectors with the highest transposition rate (Figure 2C) are
404 either based on the p1 promoter, which is a GACT track without promoter
405 activity, or proper promoters but without a RBS site indicating that a stochastic
406 Hsmar1 mRNA and/or protein production provides the highest transposition
407 rate in *E. coli*. We previously shown that OPI starts to occur when two
408 transposase dimers are present in a single cell (12). This therefore shows that
409 the expression vectors with the highest transposition rate (Bp1-, Ip1+ and
410 Bp5-) are the closest to the production of a single Hsmar1 dimer per cell
411 across the bacterial colony. Thus, the papillation assay with the Hsmar1
412 covalent dimer could be used to screen promoters to find a promoter
413 expressing on average one protein per cell across a bacterial colony. The
414 advantage of the papillation assay is that the transposition rate is quantified
415 on multiple bacterial colonies which allows a comparison of the transposition

416 rate across a population of cells. We can therefore confidently differentiate
417 between noise and real change in transposition efficiency due to OPI, as
418 shown in Figure 2C.

419

420 **Conclusions**

421 We present in this study an improvement of the papillation assay using a set
422 of constitutive promoters cloned in a one- or five-copies vector in presence or
423 absence of a ribosome binding site. This set of expression vectors gives a
424 better control of the transposase expression and the possibility to screen for
425 hyperactive or OPI-resistant transposases by using one of the optimal or high
426 expression vector, respectively. A potentially interesting approach to the
427 synthetic biology community is an experimental method based on the
428 covalently bound Hsmar1 transposase or the wild-type Hsmar1 that could be
429 used for screening weak promoters to find a promoter expressing on average
430 one or two proteins per cell, respectively.

431

432 **Methods**

433 **Media and bacterial strains**

434 Bacteria were grown in Luria-Bertani (LB) media at 37°C. The following
435 antibiotics were used at the indicated concentrations: ampicillin (Amp), 100
436 µg/ml, chloramphenicol (Cm), 25 µg/ml, and spectinomycin (Spec), 100
437 µg/ml. The following Escherichia coli strains were used: RC5024 (identical to
438 DH5α) [endA1 hsdR17 glnV44 thi-1 recA1 gyrA relA1 Δ(lacZYA-argF)U169
439 deoR (φ80dlac Δ(lacZ)M15)], RC5094 [F- araD139 Δ(argF-lac)U169 rspL150
440 relA1 flbB5301 fruA25 deoC1 ptsF25 rpoS359::Tn 10], RC5096 [F⁻ fhuA2

441 Δ(lacZ)r1 glnV44 e14-(McrA-) trp-31 his-1 rpsL104 xyl-7 mtl-2 metB1 Δ(mcrC-
442 mrr)114::*/S10 argE::Hsmar1-lacZ'-kanR*] and RC5097 (= RC5096
443 pOX38::*miniTn10-CAT*).

444

445 **Constitutive promoters**

446 Alper et al previously generated and characterized a set of constitutive
447 promoters based on *pltetO* ranging from strong down to very weak (21). We
448 select the promoters 00, jj, K, E, and W (equivalent to p2, p3, p4, p5, and p6
449 in this study) and generate p1, a featureless tract of 44 GACT repeats which
450 we represent an ideal promoter-less region (Table 1). Each promoter
451 sequence is preceded by three terminator sequences and followed by a
452 consensus or a null ribosome binding site (RBS) (and also a GACT RBS in
453 the case of p1), a transposase gene, three Flag tag and a terminator
454 sequence (Figure 1A).

455

Promoter name	Sequence	mRNA production value
p1	CTGACTGACTGACTGACTGACTGACTGACTGACT GACTGACTGACTGACTGACTGACTGACTGACTGACTG ACTGACTGACTGACTGACTGACTGACTGACTGACTGAC TGACTGACTGACTGACTGACTGACTGACTGACTGACTG ACTGACTGACTGACTGACTGACTGACTGACTGACCATATG	n.d.
p2 (00)	CAATCCGACGTCTAAGGAAACCATTATCATGACATCA ACCTATAAAAATAGGCGTATCACGAGGCCCTCTCGTCT CCACCTCAAGCTCCCTATCTAGTGATAGCGATTGACAT	0.003

	CCCTATCAGTGACGGAGATATTGAGCACATCAGCAGG ACGCACTGACCACTTTAAGAAGGAGATATACATATG	
p3 (JJ)	CAATTCCGACGTCTAAGAAACCATTATTATCATGACATT AACCTATAAAAATAGGCGTATCACGAGGCCCTTTCGTC TTCACCTCGAGTCCCTATCAGTGATAGAGATTGACCTC CCTATCAGTGATAGAGATACTGAGCACATCAGCAGGA CGCACTGACCACTTTAAGAAGGAGATATACATATG	0.159
p4 (K)	CAATTCCGACGTCTAAGAAACCATTATTATCATGACATT AACCTATAAAAATAGGCGTATCACGAGGCCCTCTCGTC TTCACCTCGAGTCCCTATCAGTGATAGGGATTGACATC CCTATCAGTGATAGAGACTGGGCACATCAGCAGGA CGCACTGACCACTTTAAGAAGGAGATATACATATG	0.299
p5 (E)	CAATTCCGACGCCTAAGAAACCATTATTATCATGACATT AGCCTATAAAAATAGGCGTACCACGAGGCCCTTTCGTC TTCACCTCGAGTCCCTATCAGTGATAGAGATTGACACC CCTATCAGTGATAGAGATACTGAGCACATCAGCAGGA CGCACTGACCACTTTAAGAAGGAGATATACATATG	0.743
p6 (W / pI tetO)	CAATTCCGACGTCTAAGAAACCATTATTATCATGACATT AACCTATAAAAATAGGCGTATCACGAGGCCCTTTCGTC TTCACCTCGAGTCCCTATCAGTGATAGAGATTGACATC CCTATCAGTGATAGAGATACTGAGCACATCAGCAGGA CGCACTGACCACTTTAAGAAGGAGATATACATATG	1

456 **Table 2: List of constitutive promoters.**

457 Nomenclature (the letters indicated between brackets are from (21)), sequence, and
458 strength of the constitutive promoters used in this study. n.d.: not determined.

459

460 **Flow cytometry**

461 RC5096 cells expressing EGFP were grown overnight at 37°C in LB medium
462 supplemented with chloramphenicol or spectinomycin. The cultures were
463 diluted in a 1:1000 ratio in fresh LB medium complemented with antibiotics
464 and grown to mid-log phase ($OD_{600} \sim 0.5$). The cells were pelleted at 6,000g
465 for 5 min, washed in 1X PBS twice, and resuspended in 500 μ l of 1X PBS.
466 Flow cytometry analysis was performed on 100,000 cells with a Beckman
467 Coulter Astrios EQ.

468

469 **Western blotting**

470 Cells containing a derivative of pMAL-c2x were grown in LB supplemented
471 with 100 μ g/ml of ampicillin at 37°C until an OD_{600} of ~ 0.5 and were then
472 induced with the required concentration of IPTG for 2 hours at 37°C. Cells
473 containing pGHM491 or pBACe3.6 derivatives were grown in LB
474 supplemented with respectively 100 μ g/ml of spectinomycin or 50 μ g/ml of
475 chloramphenicol at 37°C for the same amount of time as the induced cells.
476 Promoters' expression were analyzed by pelleting $\sim 1.5 \times 10^9$ cells. The
477 samples were resuspended in SDS sample buffer, boiled for 5 min, and
478 loaded on 10% SDS-PAGE gels. Proteins were transferred to PVDF
479 membrane, probed with an anti-Hsmar1 antibody (goat polyclonal, 1:500
480 dilution, ab3823, Abcam) followed by a horseradish peroxidase-conjugated
481 anti-goat secondary antibody (rabbit polyclonal, 1:5000 dilution, ab6741,
482 Abcam). Proteins were visualized by using the ECL system (Promega) and
483 Fuji medical X-ray film (Fujifilm).

484

485 **Papillation assay**

486 The papillation assay and the reporter strain RC5096 have been described
487 previously (Figure S1A) (18). Briefly, transposase expression vectors were
488 transformed into the RC5096 strain. It is a lac^- *E. coli* strain encoding a
489 transposon containing a promoter-less *lacZ* and a kanamycin resistance gene
490 flanked with Hsmar1 ends, which has been integrated in a silent genomic
491 locus. In absence of *LacZ*, the strain produces white colonies on X-gal
492 indicator plates. When the transposase is supplied in trans, the integration of
493 a transposon into the correct reading frame of an active gene will produce a
494 *lacZ* fusion protein. The descendants of this cell will become visible as blue
495 papillae on X-gal indicator plates. RC5096 transformants were plated on LB-
496 agar medium supplemented with 0.01% lactose, 40 $\mu\text{g/ml}$ of X-gal and either
497 50 $\mu\text{g/ml}$ of chloramphenicol or 100 $\mu\text{g/ml}$ of spectinomycin. Plates were
498 incubated 5 days at 37°C and photographed. The transposition rate is
499 determined by the number of papillae per colony or by the rate of appearance
500 of papillae on the colonies.

501

502 **Mating-out assay**

503 A chloramphenicol resistant derivative of the conjugative plasmid pOX38 has
504 been introduced in the RC5096 papillation strains to create the donor strains
505 RC5097. Briefly, RC5097 transformants and the recipient strain, RC5094,
506 were grown overnight in LB supplemented with antibiotics at 37°C. The next
507 day, respectively one and three volumes of RC5097 and RC5094 were
508 centrifuged for 5 min at 6,000x g. Each pellet was resuspended in 3 ml of
509 fresh LB, pool together, and incubated in a shaking water bath for 3 hours at
510 37°C. After the mating, the transposition events were detected by plating 200

511 μ l of each culture on LB-agar medium supplemented with tetracycline and
512 kanamycin. The number of transconjugants was obtained by plating a 10^{-5}
513 fold dilution of each culture on LB-agar medium supplemented with
514 tetracycline and chloramphenicol. The plates were incubated overnight at
515 37°C and the transposition rate determined the next day by dividing the
516 number of kanamycin-resistant cells by the number of chloramphenicol
517 resistant cells.

518

519 **Funding**

520 This work was supported by a Wellcome Trust Grant [WT093160] to RC and a
521 Biotechnology and Biological Sciences Research Council Doctoral Training
522 Program Grant [BB/J014508/1] to MT

523

524 **Availability of data and materials**

525 All data generated or analyzed during this study are included in this published
526 article and its Additional files.

527

528 **Competing interests**

529 The authors declare that they have no competing interests.

530

531 **Authors' contributions**

532 MT and RC designed the study. MT performed the experiments, analyzed the
533 data and wrote the manuscript. All authors read and approved the final
534 manuscript.

535

536 References

- 537 1. Lander ES, Linton LM, Birren B, Nusbaum C, Zody MC, Baldwin J, et
538 al. Initial sequencing and analysis of the human genome. *Nature*.
539 2001;409(6822):860-921.
- 540 2. Feschotte C, Pritham EJ. DNA transposons and the evolution of
541 eukaryotic genomes. *Annu Rev Genet*. 2007;41:331-68.
- 542 3. Aziz RK, Breitbart M, Edwards RA. Transposases are the most
543 abundant, most ubiquitous genes in nature. *Nucleic Acids Res*.
544 2010;38(13):4207-17.
- 545 4. Orgel LE, Crick FH. Selfish DNA: the ultimate parasite. *Nature*.
546 1980;284(5757):604-7.
- 547 5. Chuong EB, Elde NC, Feschotte C. Regulatory activities of
548 transposable elements: from conflicts to benefits. *Nat Rev Genet*.
549 2017;18(2):71-86.
- 550 6. Piriyaongsa J, Jordan IK. A family of human microRNA genes from
551 miniature inverted-repeat transposable elements. *PLoS One*. 2007;2(2):e203.
- 552 7. Kapusta A, Kronenberg Z, Lynch VJ, Zhuo X, Ramsay L, Bourque G, et
553 al. Transposable elements are major contributors to the origin, diversification,
554 and regulation of vertebrate long noncoding RNAs. *PLoS Genet*.
555 2013;9(4):e1003470.
- 556 8. Jangam D, Feschotte C, Betran E. Transposable Element
557 Domestication As an Adaptation to Evolutionary Conflicts. *Trends Genet*.
558 2017;33(11):817-31.
- 559 9. Tellier M, Bouuaert CC, Chalmers R. Mariner and the ITm Superfamily
560 of Transposons. *Microbiol Spectr*. 2015;3(2):MDNA3-0033-2014.
- 561 10. Claeys Bouuaert C, Chalmers R. Transposition of the human Hsmar1
562 transposon: rate-limiting steps and the importance of the flanking TA
563 dinucleotide in second strand cleavage. *Nucleic Acids Res*. 2010;38(1):190-
564 202.
- 565 11. Claeys Bouuaert C, Walker N, Liu D, Chalmers R. Crosstalk between
566 transposase subunits during cleavage of the mariner transposon. *Nucleic
567 Acids Res*. 2014;42(9):5799-808.
- 568 12. Claeys Bouuaert C, Lipkow K, Andrews SS, Liu D, Chalmers R. The
569 autoregulation of a eukaryotic DNA transposon. *Elife*. 2013;2:e00668.
- 570 13. Dawson A, Finnegan DJ. Excision of the *Drosophila* mariner
571 transposon Mos1. Comparison with bacterial transposition and V(D)J
572 recombination. *Mol Cell*. 2003;11(1):225-35.
- 573 14. Auge-Gouillou C, Brillet B, Hamelin MH, Bigot Y. Assembly of the
574 mariner Mos1 synaptic complex. *Mol Cell Biol*. 2005;25(7):2861-70.
- 575 15. Richardson JM, Dawson A, O'Hagan N, Taylor P, Finnegan DJ,
576 Walkinshaw MD. Mechanism of Mos1 transposition: insights from structural
577 analysis. *EMBO J*. 2006;25(6):1324-34.
- 578 16. Lohe AR, Hartl DL. Autoregulation of mariner transposase activity by
579 overproduction and dominant-negative complementation. *Mol Biol Evol*.
580 1996;13(4):549-55.
- 581 17. Lampe DJ. Bacterial genetic methods to explore the biology of mariner
582 transposons. *Genetica*. 2010;138(5):499-508.

- 583 18. Liu D, Chalmers R. Hyperactive mariner transposons are created by
584 mutations that disrupt allosterism and increase the rate of transposon end
585 synapsis. *Nucleic Acids Res.* 2014;42(4):2637-45.
- 586 19. Huisman O, Kleckner N. A new generalizable test for detection of
587 mutations affecting Tn10 transposition. *Genetics.* 1987;116(2):185-9.
- 588 20. Pajunen MI, Rasila TS, Happonen LJ, Lamberg A, Haapa-Paananen S,
589 Kiljunen S, et al. Universal platform for quantitative analysis of DNA
590 transposition. *Mob DNA.* 2010;1(1):24.
- 591 21. Alper H, Fischer C, Nevoigt E, Stephanopoulos G. Tuning genetic
592 control through promoter engineering. *Proc Natl Acad Sci U S A.*
593 2005;102(36):12678-83.
- 594 22. Blundell-Hunter G, Tellier M, Chalmers R. Transposase subunit
595 architecture and its relationship to genome size and the rate of transposition
596 in prokaryotes and eukaryotes. *Nucleic Acids Res.* 2018.
- 597 23. Claeys Bouuaert C, Chalmers R. A single active site in the mariner
598 transposase cleaves DNA strands of opposite polarity. *Nucleic Acids Res.*
599 2017;45(20):11467-78.
- 600 24. Cordaux R, Udit S, Batzer MA, Feschotte C. Birth of a chimeric primate
601 gene by capture of the transposase gene from a mobile element. *Proc Natl*
602 *Acad Sci U S A.* 2006;103(21):8101-6.
- 603 25. Liu D, Bischerour J, Siddique A, Buisine N, Bigot Y, Chalmers R. The
604 human SETMAR protein preserves most of the activities of the ancestral
605 Hsmar1 transposase. *Mol Cell Biol.* 2007;27(3):1125-32.
- 606 26. Miskey C, Papp B, Mates L, Sinzelle L, Keller H, Izsvak Z, et al. The
607 ancient mariner sails again: transposition of the human Hsmar1 element by a
608 reconstructed transposase and activities of the SETMAR protein on
609 transposon ends. *Mol Cell Biol.* 2007;27(12):4589-600.
- 610 27. Goodwin KD, He H, Imasaki T, Lee SH, Georgiadis MM. Crystal
611 structure of the human Hsmar1-derived transposase domain in the DNA
612 repair enzyme Metnase. *Biochemistry.* 2010;49(27):5705-13.
- 613 28. Atkinson H, Chalmers R. Delivering the goods: viral and non-viral gene
614 therapy systems and the inherent limits on cargo DNA and internal
615 sequences. *Genetica.* 2010;138(5):485-98.
- 616 29. Frokjaer-Jensen C, Davis MW, Sarov M, Taylor J, Flibotte S, LaBella
617 M, et al. Random and targeted transgene insertion in *Caenorhabditis elegans*
618 using a modified Mos1 transposon. *Nat Methods.* 2014;11(5):529-34.
- 619 30. Gayle S, Pan Y, Landrette S, Xu T. piggyBac insertional mutagenesis
620 screen identifies a role for nuclear RHOA in human ES cell differentiation.
621 *Stem Cell Reports.* 2015;4(5):926-38.
- 622 31. Bouuaert CC, Tellier M, Chalmers R. One to rule them all: A highly
623 conserved motif in mariner transposase controls multiple steps of
624 transposition. *Mob Genet Elements.* 2014;4(1):e28807.
- 625

626 **Legends**

627 **Figure 1. Characterization of the constitutive promoters.**

628 **A/** The gene of interest, Hsmar1 in this case, is fused to 3x FLAG tag on its
629 C-terminus and cloned downstream of one of six different promoters (see text
630 for more details) with a ribosome binding site (RBS) present or not. The
631 construct is located between terminator sequences (T) upstream and
632 downstream to avoid read-through transcription. To further control the number
633 of copies, the plasmid backbone is a one-copy, pBACe3.6, or five copies,
634 pGMH491, vector.

635 **B/** The promoter strength of each construct were determined by FACS after
636 cloning an eGFP gene in each vector. The number 1 to 6 corresponds to one
637 of the six different promoters. The single and five-copies vectors are
638 annotated B or I, respectively. The vector without or with a consensus RBS
639 contained a – or +, respectively. For the promoter 1, which is a repeat of the
640 GACT motif, the RBS motif can also corresponds to a GACT motif and is
641 named N (Bp1N and Ip1N). n=3.

642 **C/** Comparison of Hsmar1 expression cloned in the strongest promoters by
643 western blotting using an antibody against the C-terminus of Hsmar1.

644 **D/** Comparison by western blotting of the strongest constitutive promoters
645 against pTac promoter induced with different concentration of IPTG.

646

647 **Figure 2. Characterization of the modified papillation assay with the**
648 **wild-type Hsmar1 transposase.**

649 **A/** Representative colony of each vector expressing a wild-type Hsmar1
650 transposase. Whole plate pictures are presented in Supplementary Figure 3.

651 **B/** Quantification of the number of papillae per colony. Average \pm standard
652 deviation of the mean of six representative colonies from three independent
653 experiments.

654 **C/** Plot of the average promoter strength (as defined in Figure 1B) versus the
655 average number of papillae per colony (as defined in Figure 2B). As expected
656 from the overproduction inhibition (OPI) mechanism, an inverse power law is
657 observed between the promoter strength and the transposition rate.

658

659 **Figure 3. Expression of a covalent Hsmar1 transposase affects the**
660 **expression threshold needed to reach OPI.**

661 **A/** Schematic of the Hsmar1 monomer or covalent dimer. The difference
662 between both constructs is the insertion of a stop codon upstream of the linker
663 region in the monomer construct.

664 **B/** Representative colony of each vector expressing either an Hsmar1
665 monomer or covalent dimer transposase. Whole plate pictures are presented
666 in Supplementary Figure 4.

667 **C/** Quantification of the number of papillae per colony. The expression vectors
668 have been ordered by decreasing number of papillae per colony for the
669 Hsmar1 monomer. Average \pm standard deviation of the mean of six
670 representative colonies from three independent experiments.

671 **D/** Plot of the average promoter strength (as defined in Figure 1B) versus the
672 average number of papillae per colony (as defined in Figure 3C).

673

674 **Figure 4. Characterization by the papillation assay of different Hsmar1**
675 **mutants.**

676 **A/** Phylogenetic tree of anthropoid primates representing the apparition of
677 mutations in the Hsmar1 domain of SETMAR. All the mutations present in the
678 human SETMAR were tested by papillation assay to determine when
679 deleterious mutations for Hsmar1 transposition appeared.

680 **B/** Representative colony of pMAL-C2X expressing wild-type or mutant
681 Hsmar1 transposase. Whole plate pictures are presented in Supplementary
682 Figure 5.

683 **C/** Different Hsmar1 mutants have been tested in low, optimal and high
684 transposase expression level (Bp1+, Ip1+ and Ip6+, respectively).

685 Representative colony of each papillation plate is shown. The average
686 number of papillae per colony is indicated below the pictures. Whole plate
687 pictures are presented in Supplementary Figure 6.

688

689 **SF1. Representation of the modified papillation assay.**

690 **A/** The Hsmar1 (RC5096), which encodes a promoter-less *lacZ* gene and a
691 kanamycin resistance marker, has been integrated at a transcriptionally silent
692 locus in a lac- *E. coli* strain. In absence of transposase, the *lacZ* gene is not
693 expressed therefore the strain produces white colonies on X-gal reporter
694 plates. When the transposase is supplied in trans from a vector, if a
695 transposon integrates into the ORF of a transcribed gene, a *lacZ* fusion
696 protein will be produced. The cell's descendants will expressed LacZ and
697 therefore will appear as blue papillae on X-gal reporter plates. Black arrow,
698 promoter; open brackets, transposon ends; empty rectangle, transposase
699 gene.

700 For the mating-out assay, a chloramphenicol resistant derivative of the
701 conjugative plasmid pOX38 is introduced into the reporter strain.
702 Transposition of the reporter into the plasmid is detected by selecting
703 transconjugants after mating with a recipient strain on chloramphenicol and
704 kanamycin.

705 **B/** Example of FACS profile for each constitutive promoter expressing the
706 eGFP gene. Ip0 is the negative control with nothing cloned in the vector.

707

708 **SF2. Effect of lactose on the modified papillation assay.**

709 **A/** Representative colony of the Ip3+ Hsmar1 vector on different concentration
710 of lactose. Whole plate pictures are presented in C/.

711 **B/** Quantification of the number of papillae per colony. Average \pm standard
712 deviation of the mean of six representative colonies from three independent
713 experiments.

714 **C/** Whole plate pictures of the representative colony presented in
715 Supplementary Figure 2A.

716

717 **SF3. Characterization of the modified papillation assay with the wild- 718 type Hsmar1 transposase.**

719 Whole plate pictures of the representative colony presented in Figure 2A.

720

721 **SF4. Expression of a covalent Hsmar1 transposase affects the 722 expression threshold needed to reach OPI.**

723 Whole plate pictures of the representative colony presented in Figure 3A.

724

725 **SF5. Characterization by the papillation assay of different Hsmar1**

726 **mutants.**

727 Whole plate pictures of the representative colony presented in Figure 4B.

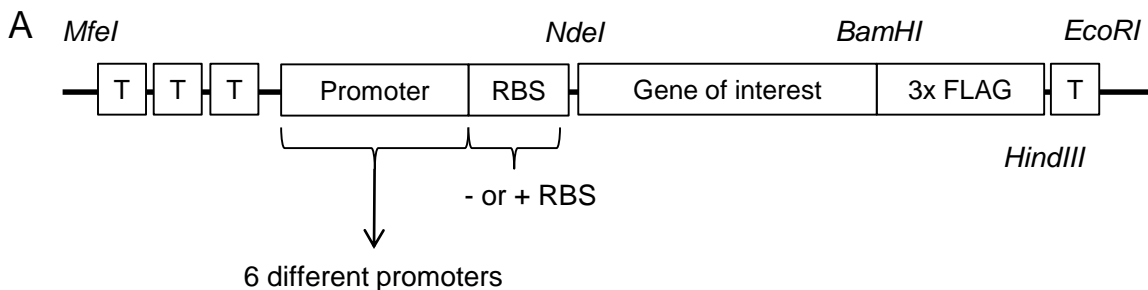
728

729 **SF6. Characterization by the papillation assay of different Hsmar1**

730 **mutants.**

731 Whole plate pictures of the representative colony presented in Figure 4C.

732



Construct in pBAC (1 copy per cell) and pIncQ (5 copies per cell)

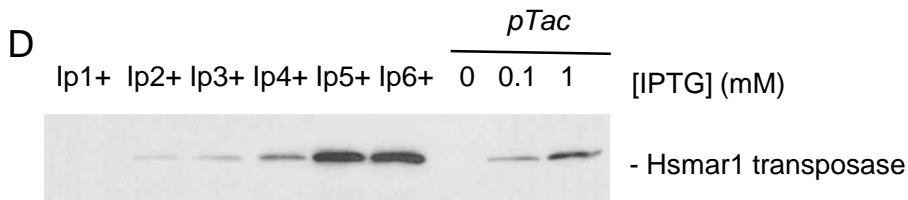
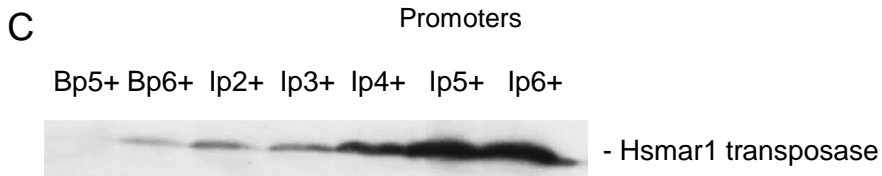
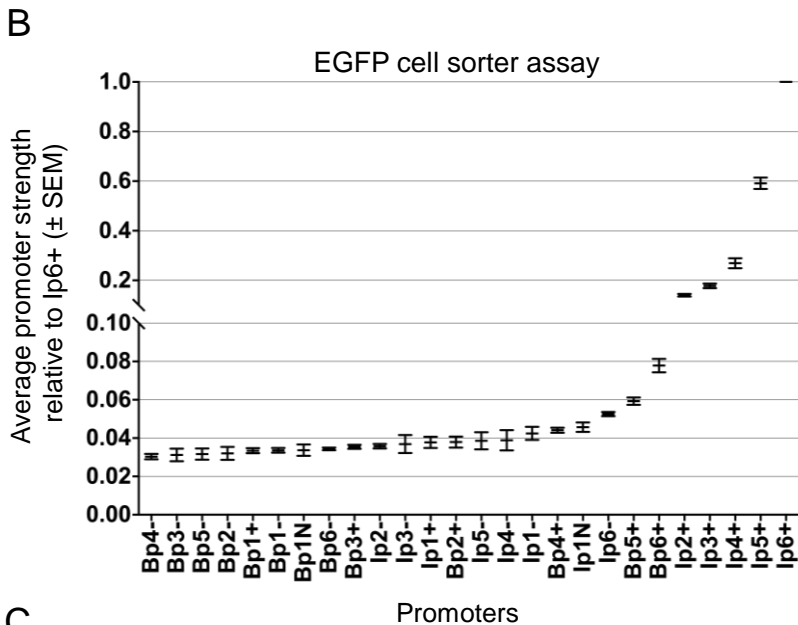


Figure 1

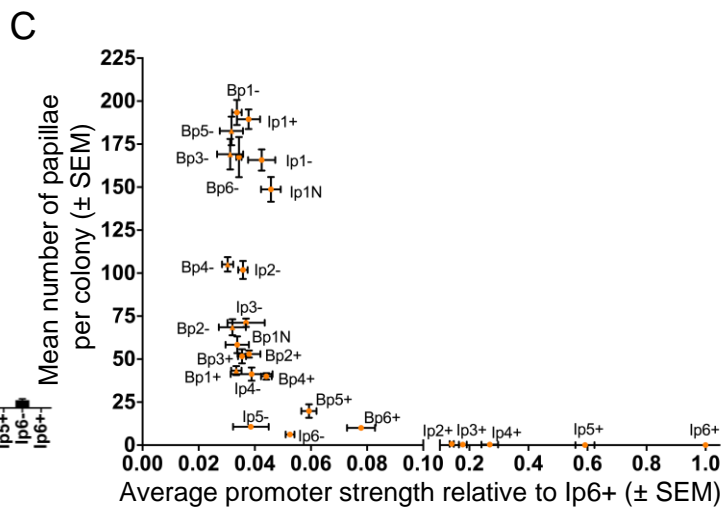
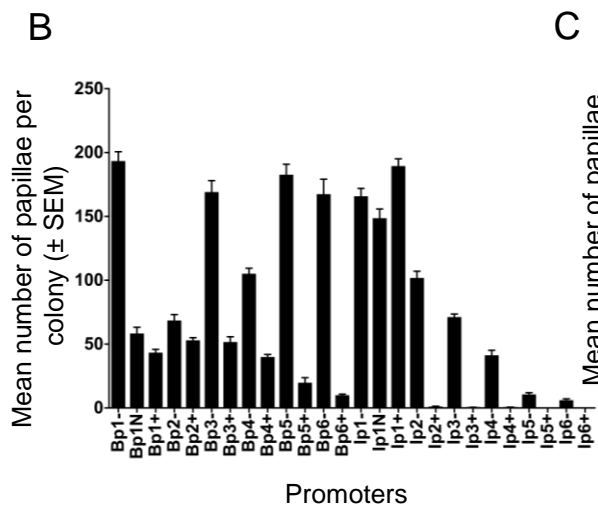
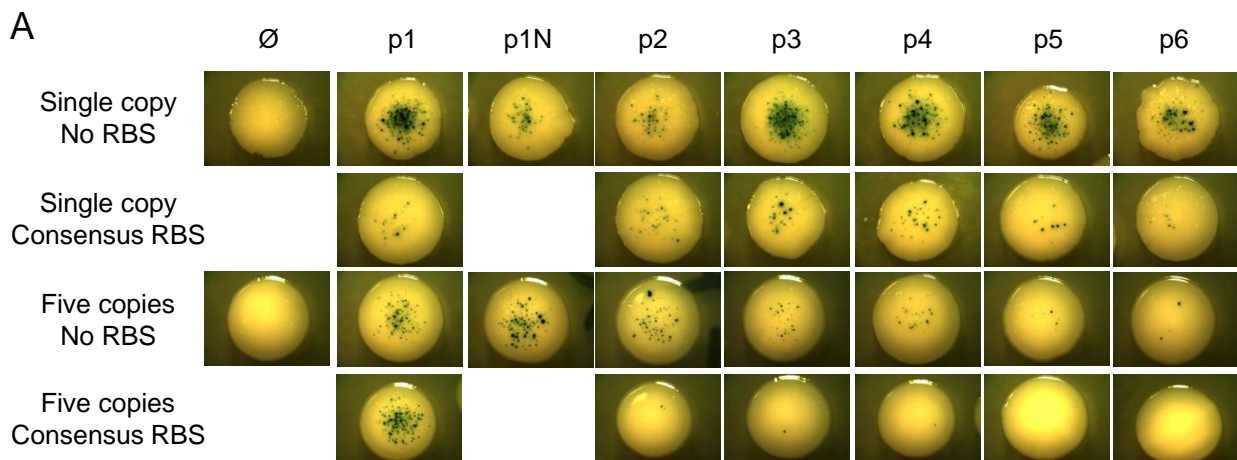
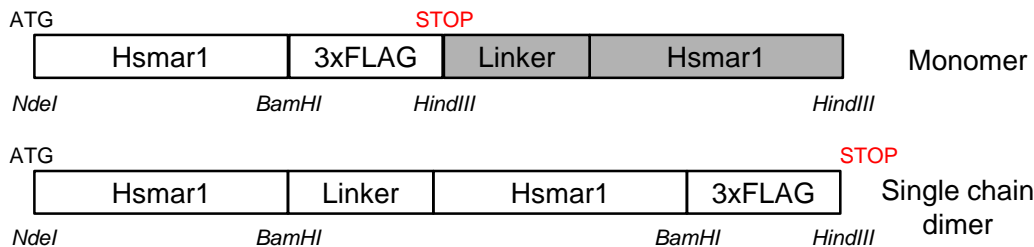
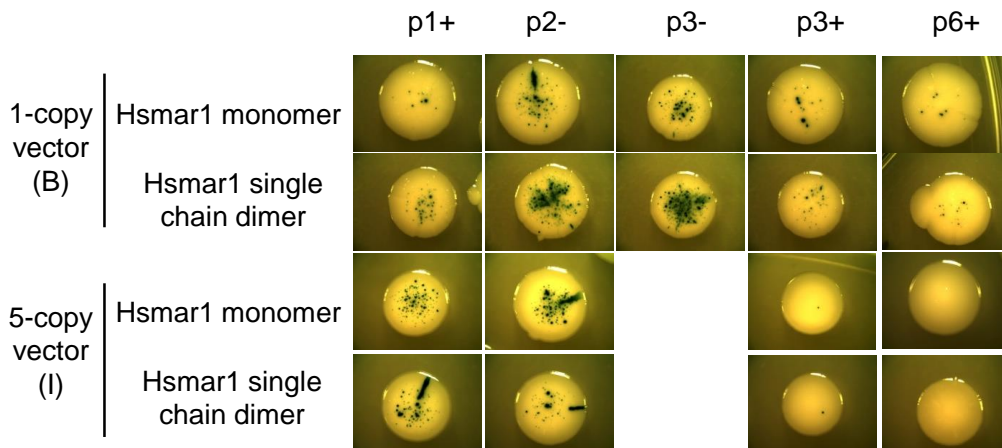


Figure 2

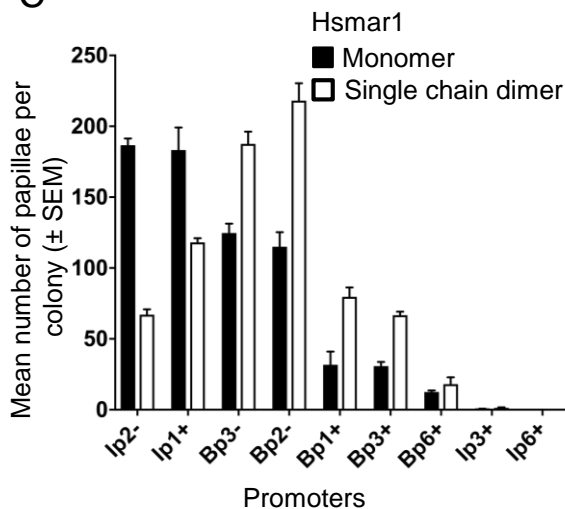
A Covalent dimer constructs:



B



C



D

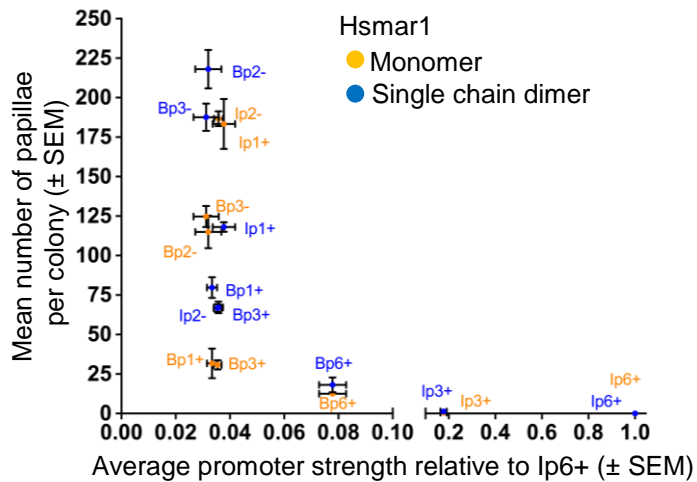


Figure 3

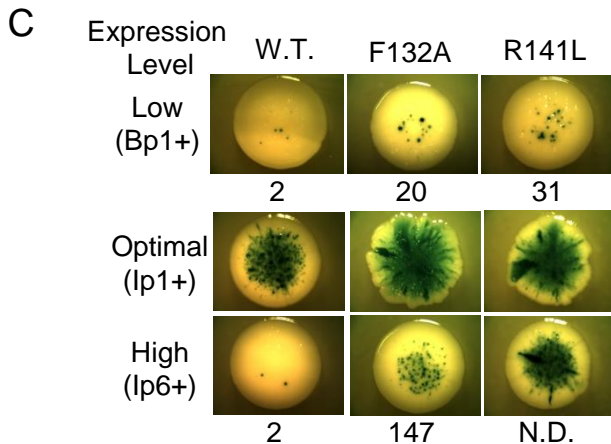
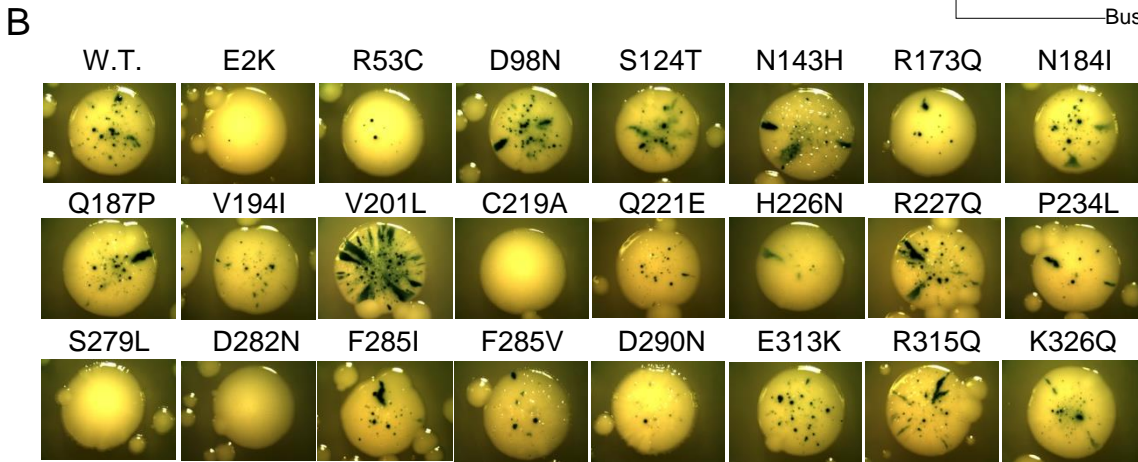
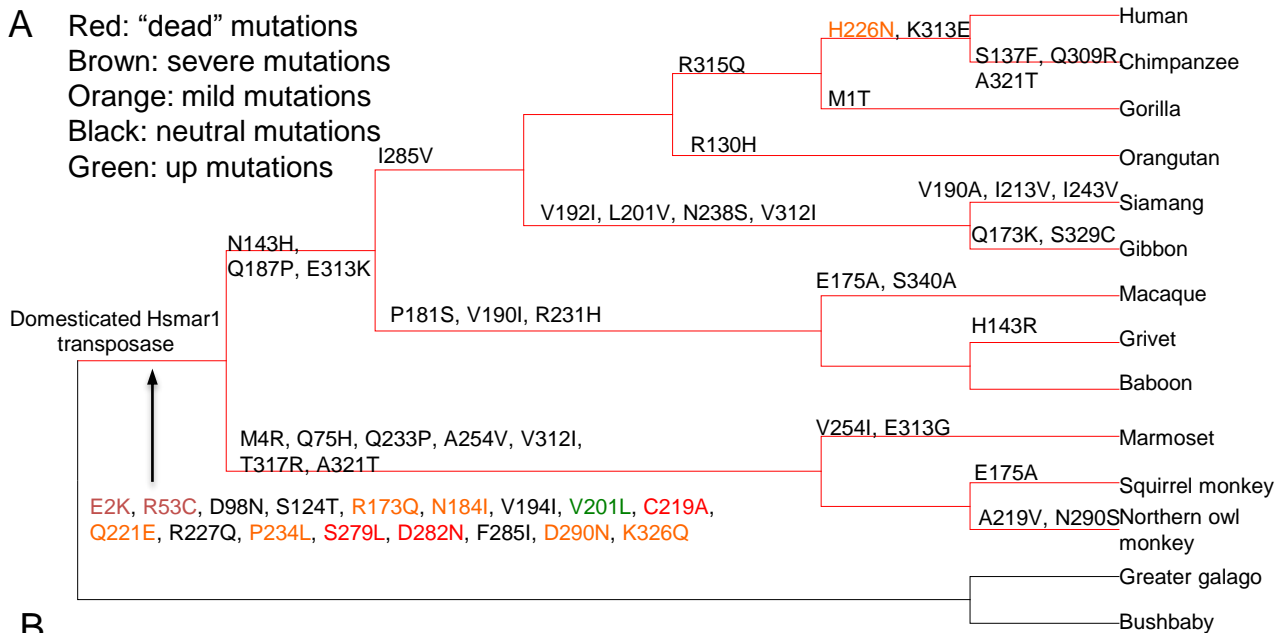


Figure 4